

Benzimidazole-loaded Halloysite Nanotube as a Smart Coating Application

Khairina Azmi Zahidah¹, Saeid Kakooei^{1,*}, Massoud Kermanioryani², Hamed Mohebbi¹,
Mokhtar Che Ismail¹, Pandian Bothi Raja¹

¹Department of Mechanical Engineering, Faculty of Engineering, Universiti Teknologi PETRONAS, Perak Darul Ridzuan, Malaysia.

²Department of Chemical Engineering, Faculty of Engineering, Universiti Teknologi PETRONAS, Perak Darul Ridzuan, Malaysia.

Received 01 December 2016; received in revised form 07 April 2017; accepted 26 April 2017

Abstract

Smart coating has been developed for the corrosion control of surfaces exposed to corrosive environment. An important step in development of a smart coating is the successful impregnation of corrosion inhibitor into the nanocontainer as a coating pigment. In this study, halloysite was used as nanocontainer to encapsulate benzimidazole as corrosion inhibitor by vacuum method. FESEM, TEM, FTIR and TGA characterization techniques were used to confirm the loading of halloysite with benzimidazole. FESEM results indicated differences between the morphology of the unloaded-halloysite and benzimidazole loaded-halloysite. TEM results confirmed that benzimidazole molecules are loaded into halloysite. FTIR result revealed there are differences in the absorbance characteristic of peaks between peak number 1000-4000 cm^{-1} for loaded and unloaded samples. It is seen that the absorbance in the loaded-halloysite is higher than unloaded-halloysite, which confirms quantity/specific functional group of molecules. TGA result showed the temperature of degradation of benzimidazole-loaded HNT was higher than pure HNT. EIS was conducted to examine the protection characteristic of the developed smart coating. From EIS results, of 1, 3, and 6 days of experimental duration, it is seen that the value of coating impedance (Z') after exposure to 3.5% NaCl environment is very high, 2.460E+07 Ω , which confirms a very good anti corrosion protection characteristic for the developed smart coating.

Keywords: benzimidazole, halloysite nanotube, nanocontainer, smart coating

1. Introduction

Corrosion is one of the most severe issues in oil and gas industry. There are many ways to control internal and external of a metal from corrosion degradation, which can be categorized in to: application of cathodic protection, application of coating, injection of corrosion inhibitor, and alteration of medium corrosivity. Amongst this, coating has been widely used in the past as an effective means to control corrosion. The efficiency of the coated surface in terms of complete surface coverage is generally not sufficient for applications in aggressive and extreme environments, such as in coastal areas that could be seen the green corrosion or internal corrosion of a vessel [1]. Therefore, smart coating has been developed to solve that problem. Smart coating is a development of coating by converting the coating material to be more responsive, adaptive, and effective to prevent substrates from corrosion [2]. Functioning inhibitors, which are directly added to the coating, based on the chemical properties

* Corresponding author. E-mail address: saeid.kakooei@utp.edu.my

Tel.: +601-7-4958196

of such inhibitors could be allowed the weakening in the ability of corrosion protection of the coatings [3]. Meanwhile, the direct addition of corrosion inhibitors to the coating is ineffective due to the corrosion inhibitors are easily dissolve in the surrounding environment, which can leave a blank space on the coating that reduce the effectiveness of the barrier properties of the coating [4]. In addition, the inhibitor also easily reacts with other substances in liquid paint.

The requirement to add the inhibitor in directly to the paint leads to a technology which is used in container or capsule to encapsulate the inhibitor. The method does not require a large amount of inhibitor since a low concentration inhibitor can be extremely effective and only released on damaged area [1]. In addition, the long, thin, and tubular systems of nanotubes are very suitable as nanocontainer. Therefore, nanotubes are appropriated candidate to be used as a nano container for inhibitor. Several studies on the use of nanotubes as nanocontainer have focused on boron nitride nanotubes (BNNT) and carbon nanotubes (CNT). However, both of them must be produced in a bulk form that makes them expensive. In addition, CNT is a substance that is toxic and low availability [5-6]. Halloysite (will be abbreviated as HNT) is an economical nanotube, biocompatible, non-toxic, high mechanical strength, and abundant availability. HNT is reported significantly increase the release time of the inhibitor in the aqueous environment [6-7]. Thus, HNT has a big chance as a nanocarrier for active agent. Besides, benzimidazole is the best candidate as corrosion inhibitor. Benzimidazole is a low toxicity heterocyclic organic compound which is consisting of a combination of benzene and imidazole. Benzimidazole and its derivatives are known to be good and excellent corrosion inhibitor for metal and alloys [8-10]. Thus, the aim of this work is to study the use of HNT as a nanocontainer in loading of benzimidazole as the corrosion inhibitor.

1.1. Coating

The development of the strategy for corrosion prevention and inspection in the pipeline is very important for safety and cost effectiveness of operation of the pipeline. In the context of pipeline protection, many efforts have been placed on both external and internal of the pipeline. For the external corrosion protection, there has been considerable effort to protect and maintain the external surface of the onshore and offshore pipelines from corrosion by application of protective coating and cathodic protection. For the protection of internal surface of the pipeline, injection of corrosion inhibitors has been a primary method in control of corrosion. However, the continuous injection of corrosion inhibitors, especially in high dosage, is costly. Thus, it is a need to design a protection system to reduce the inhibitor cost [11].

Coating is a material which contains synthetic resin or inorganic silicate polymer that forms continue film on the metal surface [12]. The continue film will limit the contact between environment and metal surface. Then, it becomes resistant to the environment. The coating should have the following characteristics in order to prevent corrosion: (1) good adhesivity with a metal surface. (2) Minimum discontinuity in coating (porosity). (3) High resistance to electron transfer. (4) Sufficient thickness (the thicker the coating, the better the corrosion resistance). (5) The low diffusion rate of the ions (such as Cl^-) and H_2O . Based on corrosion resistance, coating is divided into several types, namely barrier coatings, conversion coatings, cathodic coatings and anodic coatings [12].

For internal coating of pipeline, improvement in flow efficiency by the means of reducing friction is the main reason of the use of that coating. The utilization of internal coating of continues perfect film, can improve corrosion protection and pre-commissioning operations and pigging operations. The efficiency enhancement is achieved by reducing internal surface roughness, which means decreasing friction in the pipe by reducing surface roughness. In addition, the presence of free water in the system is one of the causes of internal corrosion in the pipeline. Good coating system will provide an effective barrier against corrosion. Pigging frequency requirements may be reduced by the use of internal coating of a pipeline. Selecting coating

materials is influenced by environmental condition and service requirements of the pipeline. There are some types of coatings, one of the main types of coating for the internal coating material are epoxies, urethanes, and phenolic. The epoxy-based material commonly used for internal coating because it has a pretty good hardness property, resistant to water, good flexibility, resistant to chemicals, and good adhesion to the substrate [13].

1.2. Smart Coating

The need for the efficient and low-cost corrosion control has led to the development of the corrosion prevention technologies of smart coatings. Smart coatings are coatings that are changing their nature in response to stimuli from the environment. Responsive, adaptive and active are the appropriate term for smart coatings. As indicated, smart coatings with the response to the environment, makes them very demanding in variety of potential applications. Smart coatings can be divided into several types, namely self-cleaning, self-healing, microcapsule-healing, and anti-corrosion coatings. Smart anti-corrosion coating is believed to trigger the dismissal of corrosion that occurs in the system. The concept of self-healing anti-corrosion coating will occur after the wound healing process. The treatments that do not fit with the wound will cause inflammation which corrosion will spread under the coating. That case triggers the use of inhibitors in coating (Fig. 1). The use of inhibitors in coating can be done by various methods, from simple to complex one. The applied method depends on factors such as: the solubility of inhibitors, chemical costs, and technical difficulties. Smart coatings, which are currently developed, are nanocoating. Nanocoating is the application of nanotechnology to the techniques of corrosion prevention, where the nanoscale material has unique properties on the chemical, physical, and physicochemical. Nanocoating is formulated by the addition of nanoparticles in the coating which will then enhance the features of the coating [2].

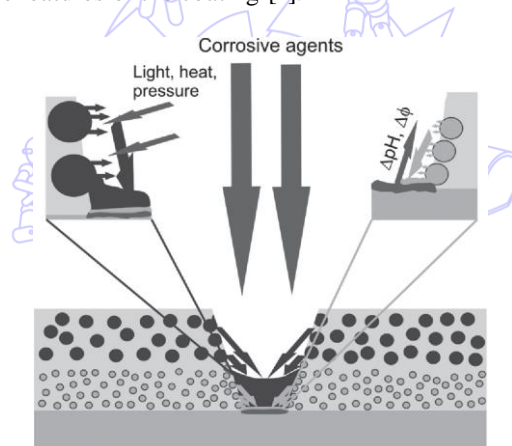


Fig. 1 Schematic of Inhibitor loaded in micro/nanocontainer as a self-healing coating [14]

For self-healing and nanocoating, microencapsulation technology is being developed nowadays. The word encapsulation derived from the Latin "en" which means inside and "capsule" which means a small box. Literally to encapsulate means putting something into a small box. The word microencapsulation means encapsulate particle with the size of 1-999 micrometer (10^{-6} - 10^{-3} meters). But in reality, the term is used to insert a nanometer up to millimeter-sized particles. The reason to do encapsulate particles is to change or prevent direct interaction between the encapsulated materials to the external environment. The impact of the capsule with a smaller size will boost dispersity and encourage microtechnology to nanotechnology in this encapsulation technology [15].

1.2.1. pH-Sensitive Micro/Nanocontainer

One of the mechanisms for releasing active agent from micro/nanocontainer is triggered by pH changes of the surrounding. Effective nanocontainers such as micelles or vesicles are naturally used in biological system. However, lacking mechanical stability limits their applications. Therefore, it has been mainly development in polymer nanocontainer due to its high stability

[16]. The approach of polyelectrolyte nanocapsules as mimetics of virion particles was largely inspired by nanocontainer system with pH-controlled which are accessible to inner cavity. Polyelectrolyte is very sensitive to the physicochemical conditions of the surrounding such as ionic strength, pH, and the presence of multivalent ions. Therefore, to prevent that problem, water-soluble polymer hollow spheres that composed by covalently crosslinked polyelectrolyte shells are used. In carboxylate group nanocapsules based, there are separations which continue to increase with increasing pH. As a result of electrostatic bonding repulsion between the increased of charged carboxylate anion along the polymer chain, shells of these particles must swell with increasing pH. Based on research conducted by Marc Sauer et al., (2001), the particle radius increased from the previous 45 nm at $\text{pH} < 4$ to 195 nm at $\text{pH} > 9$ [16].

Sergio Simoes et al., (2003) discussed the pH-sensitive liposomes. pH-sensitive liposomes are used to deliver anticancer drugs, antibiotics, antisense oligonucleotides, ribozymes, plasmids, proteins, and peptides. The concept of pH-sensitive liposomes appears based on the fact that the virus is currently developing a strategy to take advantages of the acidification of the endosomal lumen to infect cells. This is based on, the observation that some pathological tissues showed an acidic environment compared to normal tissues. When the physiological pH-stable liposome has been formed, the acidification triggers the protonation of the carboxylic group of amphiphilic and reduces the stabilization effect. This will trigger liposomal destabilization, since in these conditions PE (phosphatidylethanolamine) molecules return to form hexagonal phase [17].

Tse-Ying Liu and Yi-Ling Lin (2010) conducted research on the chitosan-based hydrogel for encapsulating poorly water-soluble drugs. CHC hydrogel can show pH-sensitive properties because they contain acid (COOH) and base (NH₂) functional group (3). Swelling or water absorption on pH-sensitive hydrogels are determined by the ionization of functional group of hydrogel and intermolecular volume for water, also relies on macromolecular structure, the state of water, the hydrophobic/hydrophilic characteristic, and electric charge [18].

Jian Qian and Cory Berkland (2015) published the results of their work on pH sensitive triblock copolymer. In that study, capsules were deformed if the pH is reduced to below 6. By reducing the pH from 7.3 to 6.1, the size of the capsules was increased from 150 to 350 nm. The enhancement of the capsules' size was because of the swelling of the capsules shells which is a result of partial ionization of amines from one block polymer [19].

Further research on curcumin gelatin microspheres encapsulation was performed by Joaquin Gomez Estaca et al., (2015). The results showed that curcumin stability was against pH. In pH 5 condition, curcumin stability was higher compared to the conditions of pH 7 [20]. Research conducted by Madhusudana K. Rao et al., (2014) also discussed the curcumin encapsulated by a pH-sensitive gelatin as an anti-cancer drug delivery. The results showed that the average diameter of nanocapsules increased slowly when the pH was increased from 1.2 to 5.0 and increased rapidly when the pH was increased from 5.0 to 8.5. This can be explained by the ionization of the carboxylic functional groups, which are responsible for the increasing in swelling of the nanocapsules. The interaction between ion COO⁻ could increase the capacity of swelling of the nanocapsule. At higher pH, the chain was rejected by the carboxylate ion concentration in the solution and the charge was minimized by the expansion [21, 22].

Compared with the conventional medicine, drug delivery systems have several advantages, such as can control or sustain drug release kinetics, improve patient compliance, can modify the external shells, have specific nanomaterial properties and low toxicity [23, 24]. Among nanoparticles, pH-sensitive nanoparticles were the most widely used for cancer therapy. pH-sensitive nanoparticles which were designed to be active at low pH will release the drugs loaded into the acidic extracellular space of solid tumors. In that process, the encapsulated will be stable during the circulation of blood until the passive nanoparticles accumulate in the region of the tumor through the EPR effect. Research conducted by Yongjiu Lv et al., (2016) showed that the release of the RES (drug) of the RES-PNP (drug-loaded nanocontainer) was significantly faster at pH 5 than at pH 7.4 [25].

Another study which was also conducting studies on pH-sensitive nanocapsules, using a polymer nanocapsule showed that at pH 3, nanocapsules assumed on the condition of "closed" while at pH 9, it was assumed "open". In protonated form, shell was in glassy conditions with the features strong diffusion barrier against fragrance. By increasing the pH value until 9, carboxylic acids occurs deprotonated and polyelectrolyte shell will be created with increased hydrophilicity [26].

1.3. Organic Corrosion Inhibitor

On the application of organic compounds as corrosion inhibitors, they can act as a cathodic, an anodic, or both cathodic and anodic. But in general, the organic corrosion inhibitors will absorb on the surface of the metal and will initiate the formation of film (Fig. 2). These corrosion inhibitors will form a protective film with the metal ion on the metal surface, which would be act as a barrier between the metal and the solution or the external environment. Corrosion inhibitor molecules that have a high affinity to the metal surface show the inhibition process is effective and have low risk to the environment [27].

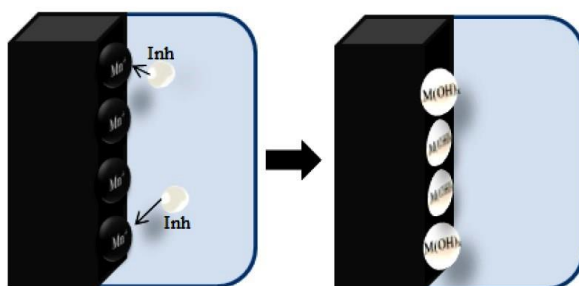


Fig. 2 Illustration of organic inhibitors effect and their mechanism of action through absorption on the metal surface [27]

Organic corrosion inhibitor contains Oxygen (O), Nitrogen (N), Sulphur (S) atoms. Based on the ability of the atoms to form covalent coordination bonding, the efficiency of corrosion inhibitor will increase as follows: corrosion inhibitor containing O atom < corrosion inhibitor containing N atom < corrosion inhibitor containing S atom. In general, inhibitors which have both atom O and N showed ability as a better inhibitor than the compounds that only have O or N atom. Among the various nitrogen compounds, azole derivatives have been regarded as environmentally friendly chemicals [28].

2. Methodology

2.1. Materials and Instrumentations

HNT was purchased from Sigma Aldrich. Benzimidazole was also obtained from Sigma Aldrich. The characterization of all samples was done by Field Emission Scanning Electron Microscopy (FESEM, SUPRA 55VP, Carl Zeiss AG, Germany) to observe the morphology and external surface of HNT. For imaging, voltage was accelerated at 0.1 - 30 kV. Transmission Electron Microscope (TEM, LIBRA 200FE, Carl Zeiss AG, Germany) was used to observe inner morphology and to measure outer and inner diameter of HNT. Voltage was accelerated at 200 kV. To investigate the functional group of the compound, Fourier Transform Infrared Spectroscopy (FTIR, Spectrum One/BX, Perkin Elmer Inc.) was used. Thermogravimetric Analysis (TGA, Perkin Elmer Inc.) was used to evaluate the loading efficiency of benzimidazole into HNT lumen.

2.2. Benzimidazole loading

First, 10mg of benzimidazole was dissolved into 15ml of acetonitrile (should be a space between 10 and 15). Then, the solution was stirred vigorously by magnetic stirrer at room temperature for 1 hour. HNT was added to the solution and stirred for 48 hours at room temperature. A solution containing HNT and benzimidazole then transferred into a vacuum rotary evaporator to remove acetonitrile and load benzimidazole into HNT internal lumen.

2.3. Corrosion Testing

To evaluate corrosion protection of benzimidazole-loaded HNT and uncoated specimen, Electrochemical Impedance Spectroscopy (EIS) testing was conducted on a coated sample with smart coating and bare specimen for the reference. ACM Gill 12 Weld Tester instrument was used. EIS experiment were taken from using a three-electrode cell with an Ag/AgCl as the reference electrode, the coated/uncoated sample as the working electrode, and stainless steel as the counter electrode or auxiliary electrode. The coated sample was prepared by mixing benzimidazole-loaded HNT with epoxy resin and applied on the metal substrate by one layer coating. The coating thickness after curing (dry film thickness) was measured to be between 270-295 μm . The corrosion environment was carried out by 3.5wt% of NaCl.

3. Results and Discussion

3.1. Benzimidazole-Loaded HNT Analysis

HNT falls into the same category as kaolinite from chemical composition views. However, the difference lies in the water content, thus, the chemical formula of HNT as $\text{Al}_2(\text{OH})_4\text{Si}_2\text{O}_5 \cdot n\text{H}_2\text{O}$ (2, 4, 2, 5, 2 should be subscript). The hydrated shape of HNT, when $n = 2$, called "HNT-10(\AA)", wherein there is a layer of water between the layers [29]. In general, HNT length lies in the submicron range up to a few microns; even some of them are more than 30 micrometers [30]. Besides, the external diameter is approximately 30-190 nm and the internal diameter is 10-100 nm [29]. The loading mechanisms of substances into HNT are divided based on the nature of the compound. To entrap hydrophilic molecules, HNT was mixed with a saturated solution of the active agent and then exposed to a high vacuum condition. For materials with high solubility, they can be loaded by blending them with a polymeric material that is compatible with the active agent, such as polyvinylpyrrolidone. Material with a low melting point can be loaded in liquid form [5].

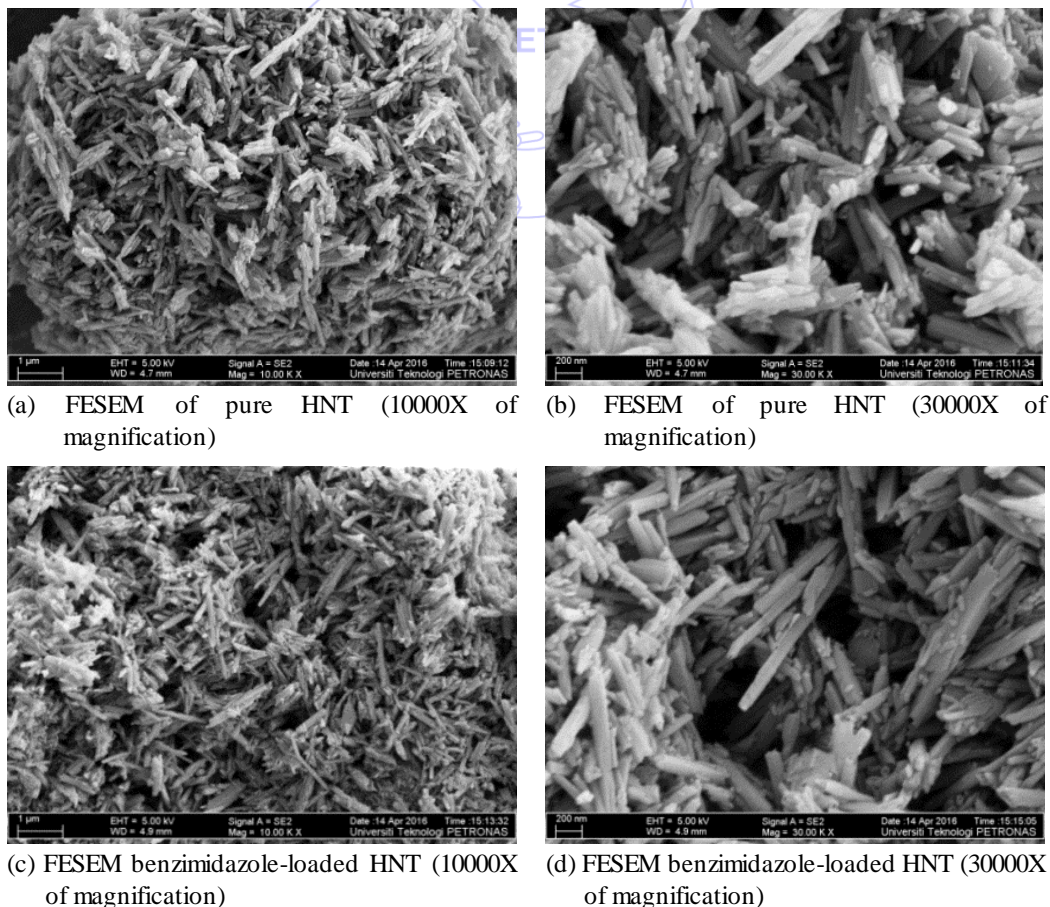


Fig. 3 FESEM of Pure HNT and Benzimidazole loaded HNT

Fig. 3 (a-b) show the FESEM results from pure HNT samples and Fig. 3 (c-d) show benzimidazole-loaded HNT samples. The FESEM results clearly show the tubule shape of HNT. More impurities are shown in Fig. 3 (d) than Fig. 3 (b). It can be assumed that the impurities are the benzimidazole particles. Fig. 4 exhibited TEM result of pure HNT and benzimidazole-loaded HNT. Fig. 4 (a-b) which are the TEM result of pure HNT show the clearly empty lumen of HNT. The inner and outer diameter can be known from TEM result. The outer diameter of HNT is $\pm 50-90\text{nm}$, while the inner diameter is $\pm 10\text{nm}$. In Fig. 4 (d), it can be seen there is benzimidazole molecule. On the other hand, in Fig. 4.c there are a lot of benzimidazole molecules outside the inner lumen of HNT. This can be caused by several factors, including factors that affect the current implementation of the experiment such as time, temperature, loading cycle, amount of HNT and corrosion inhibitor, and the solvent of corrosion inhibitor. Besides that, there are also external factors that can affect the results of characterization, such as considerable time lag between the implementation of the experiment with the characterization which can be effect to the releasing of corrosion inhibitor from the HNT lumen.

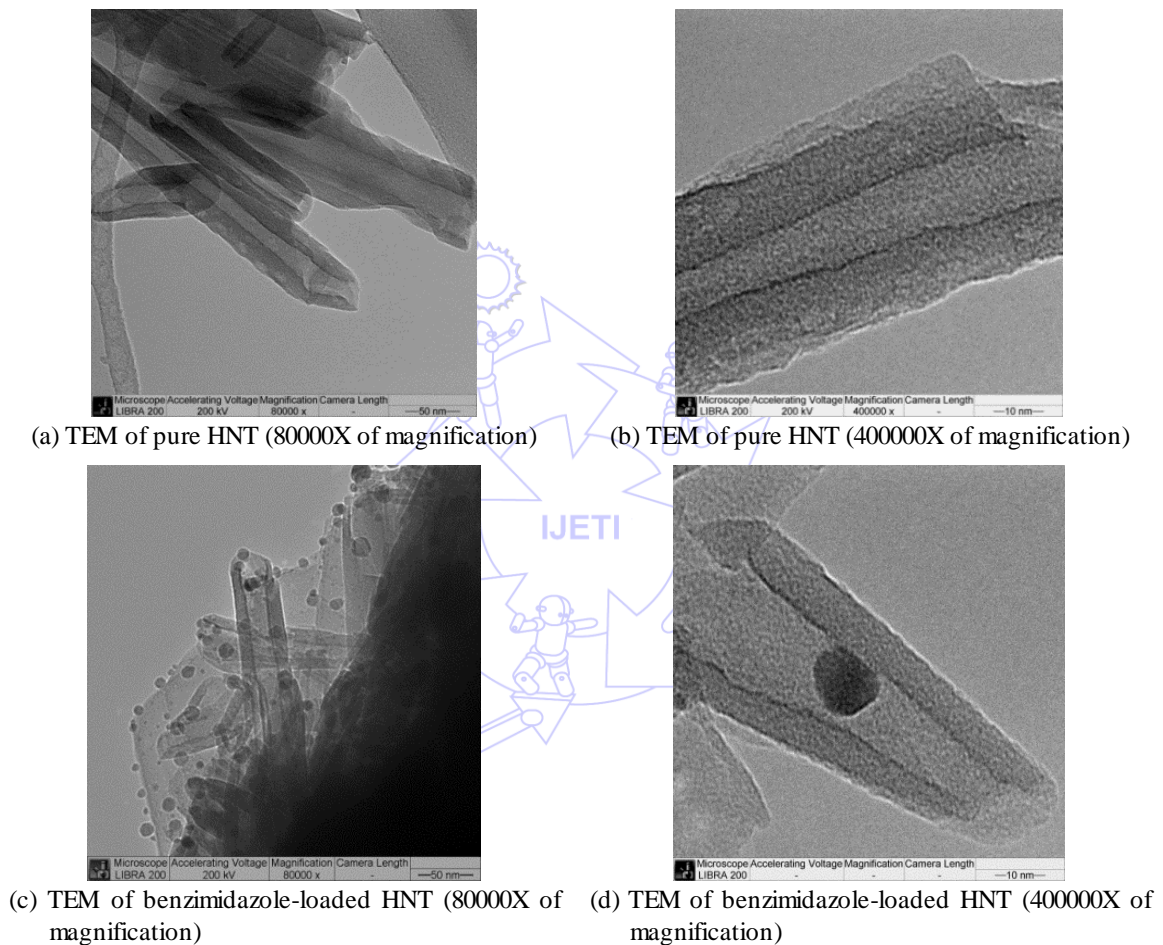
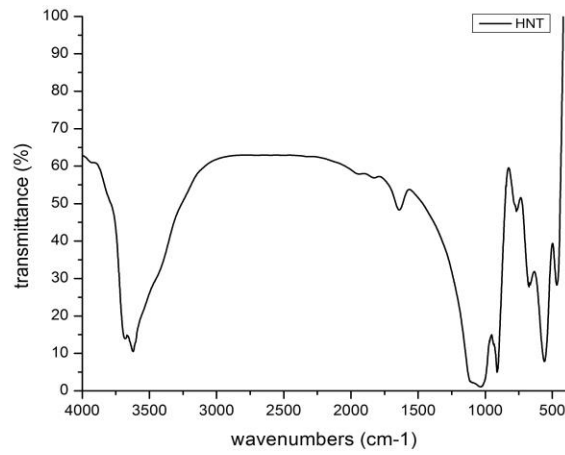
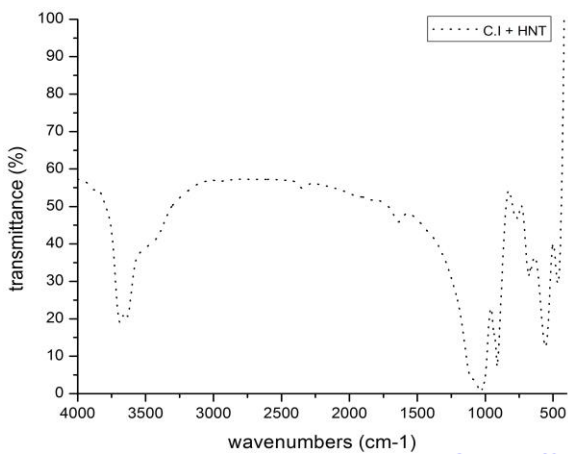


Fig. 4 TEM of pure HNT and Benzimidazole loaded HNT

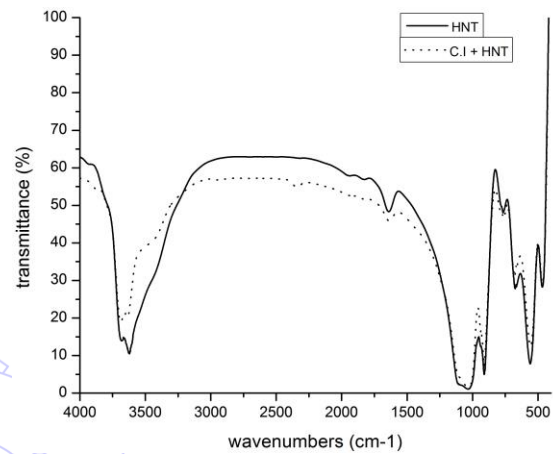
Fig. 5 shows FTIR result of (a) pure HNT, (b) benzimidazole-loaded HNT, and (c) mixgraphs a and b. From FTIR result, there are peaks in pure HNT graph at 3620.24cm^{-1} , 1640.11cm^{-1} , 1033.99cm^{-1} , 911.94cm^{-1} , 767.92cm^{-1} , 673.96cm^{-1} , 559.68cm^{-1} , 466.74cm^{-1} peaks in pure HNT graph. While in benzimidazole-loaded HNT graph, there are peaks at 3687.5cm^{-1} , 2342.39cm^{-1} , 1636.85cm^{-1} , 1041.01cm^{-1} , 911.49cm^{-1} , 760.04cm^{-1} , 679.86cm^{-1} , 567.47cm^{-1} , 466.44cm^{-1} . The 3620.24cm^{-1} and 3687.55cm^{-1} peaks were defined to O-H stretching vibration due to the inner surface of O-H groups of HNT and assigned to Al_2OH . The absorption bands at 1640.11cm^{-1} and 1636.85cm^{-1} were stipulated as interlayer water. The Si-O stretch was indicated by 114.10cm^{-1} and 1107cm^{-1} . The absorption bands at 1033.99cm^{-1} and 1041.01cm^{-1} were defined to Si-O-Si stretch. The 911.94cm^{-1} and 911.49cm^{-1} were assigned to the inner surface hydroxyl group. The O-H translation vibration of HNT O-H units was assigned by 767.92cm^{-1} and 760.04cm^{-1} . The vibration of Al-O-Si at 559.68cm^{-1} and 557.47cm^{-1} confirm the existence of that functional group. The band observed at 466.74cm^{-1} and 466.44cm^{-1} was due to the vibration of Si-O-Si.



(a) FTIR Result of Pure HNT



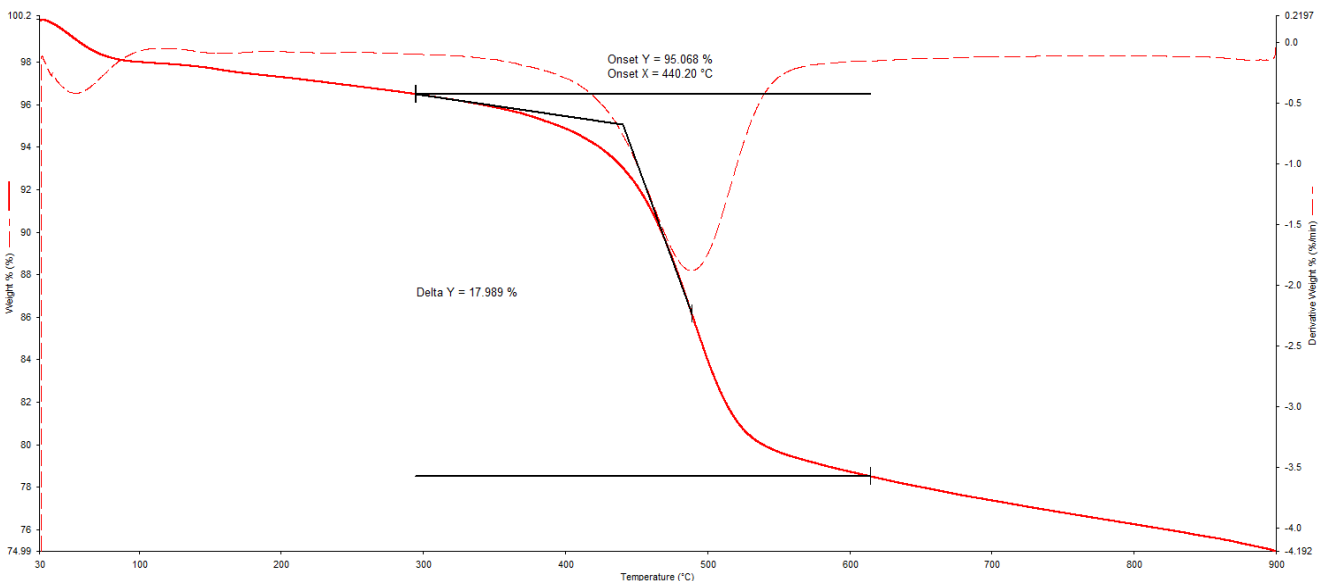
(b) FTIR Result of Benzimidazole-loaded HNT



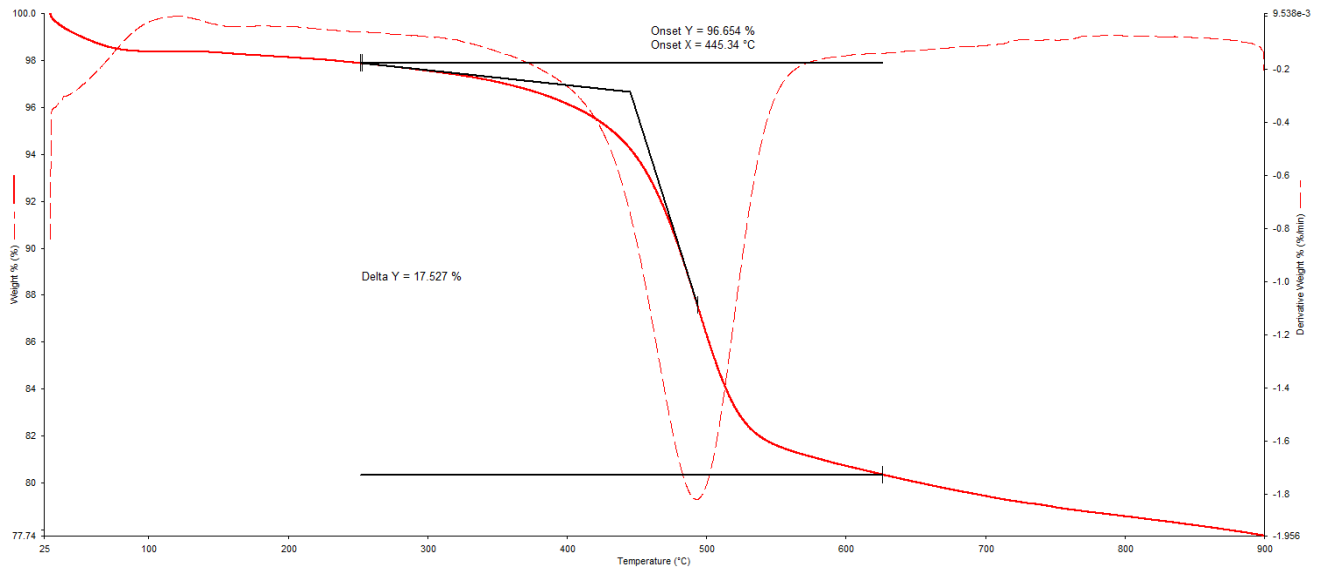
(c) FTIR Result of Pure HNT and benzimidazole-loaded HNT

Fig. 5 FTIR Result of Pure HNT and Benzimidazole-loaded HNT

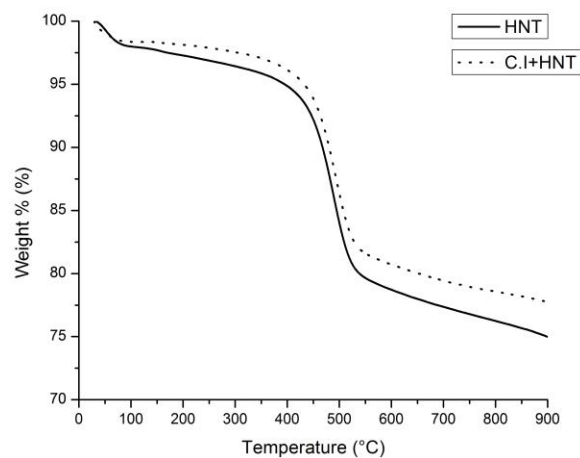
TGA testing aims to estimate the efficiency loading of corrosion inhibitor into HNT. Fig. 6 shows TGA graph of pure HNT (a), benzimidazole-loaded HNT (b), and merge of both graph (c). Figs. 6 (a) and (b) show the temperature of degradation on benzimidazole-loaded HNT (445°C) was higher than pure HNT (440°C). Temperature of degradation can be determined as thermal stability of the sample. The enhancement of thermal stability of benzimidazole-loaded HNT can be due to loaded or encapsulated benzimidazole into HNT lumen. However, the enhancement was not significant, it caused by the amount of benzimidazole in that mixture was too small. Thus, the benzimidazole which loaded into HNT lumen will be less than that.



(a) TGA curve of Pure HNT



(b) TGA curve of Benzimidazole-loaded HNT



(c) TGA curve of Pure HNT and benzimidazole-loaded HNT

Fig. 6 TGA curve of Pure HNT and benzimidazole-loaded HNT

3.2. Electrochemical Impedance Spectroscopy (EIS) Analysis

Figs. 7 and 8 show the nyquist plot for day 1, 3, and 6 of immersion of bare metal and benzimidazole-loaded HNT coated (C.I+HNT) samples. From the graph the Z' value in low frequency is measured to be 364.68Ω and 8922300Ω for bare metal and C.I+HNT respectively. From Figs. 7 and 8, a significant difference in impedance value of C.I+HNT coated and uncoated specimens are seen. The low value of impedance in uncoated specimen is due to lack of protective film on the surface of the specimen, where the C.I+HNT coated specimen have much impedance value. The measurement taken from 1, 3, and 6 days post exposure to the solution reveals the same trend for all the impedance values. The higher the impedance/resistance value the better the coating protection characteristic. The impedance values measured from this experiment is in line with the values reported by some literatures for specimens coated with only epoxy and no HNT with the similar film thickness as reported by Jin Tao Zhang et al., (2004) [31], Sami Masadeh (2005) [32], and M. Behzadnasab, et al., (2011) [33]. This confirms that the corrosion protection nature of the coating has been retained during the loading of the benzimidazole. The high impedance value of coating may be due to the fact that benzimidazole-loaded HNT has functioned as filler in the empty spaces of the epoxy matrix, which subsequent can increase the corrosion protection characteristic of the coating.

Fig. 8 shows the nyquist plot by sample condition, (a) bare metal and (b) benzimidazole-loaded HNT/epoxy. The graph showed the differences in the size of semicircle on day by day for each sample. The nyquist plot of bare metal sample 6 days from the immersion shows approximately the same size of semicircle as for the data obtained from 3 day post immersion exposure. In

the case of the non-coated bare specimen, the increase in the impedance value from day 1 to days 6 can be due to formation of an oxide layer on the surface. For the coated specimen, the semicircle becomes smaller as the time of the experiment increases, which can be related to the water uptake.

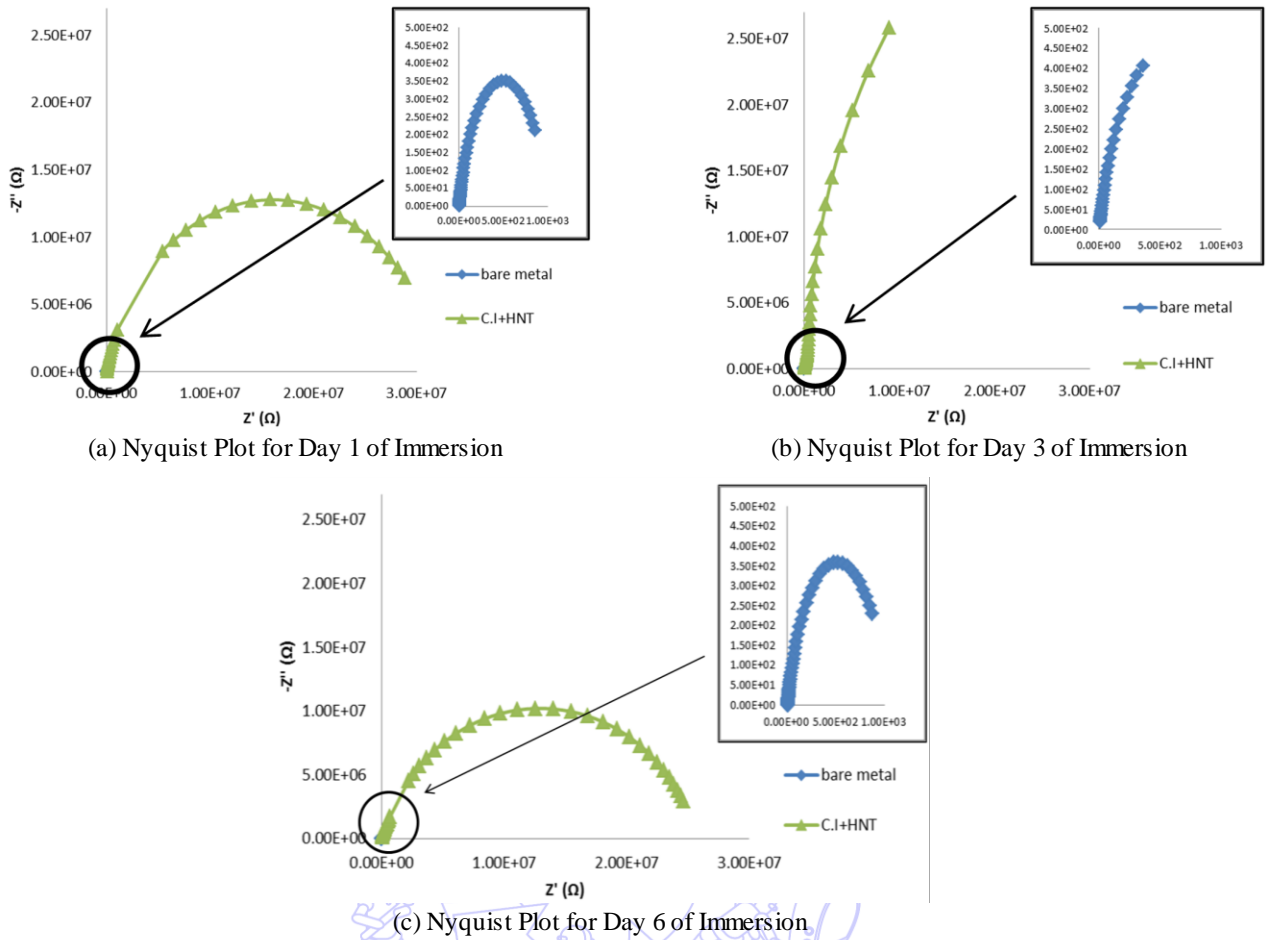


Fig. 7 Nyquist Plot for (a) Day 1, (b) Day 3, (c) Day 6 of Immersion

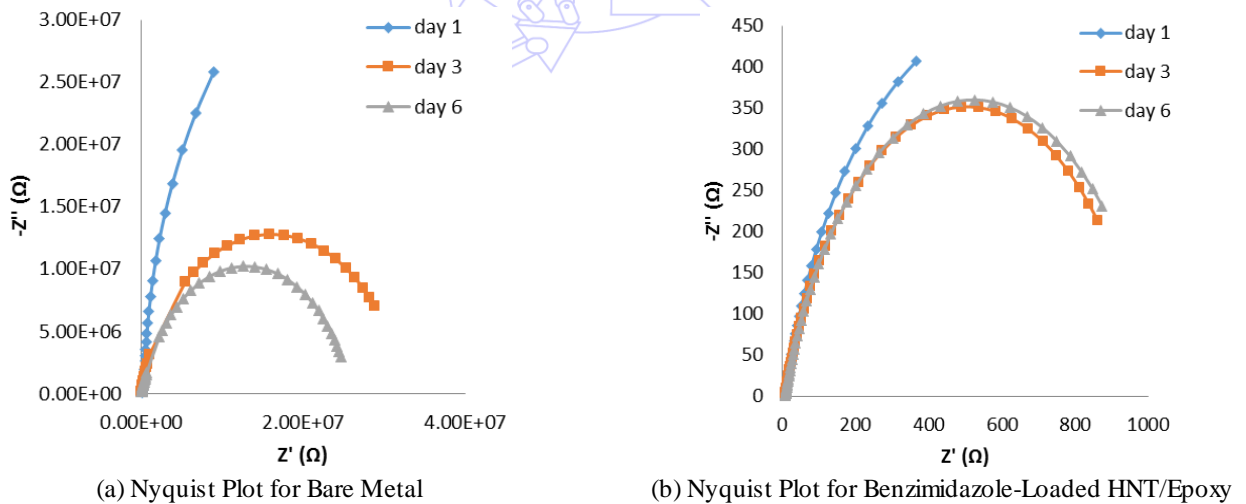


Fig. 8 Nyquist Plot for Bare Metal and Benzimidazole-Loaded HNT/Epoxy

4. Conclusion

Based on the results, the vacuum method can be successfully used for loading particles (in this case benzimidazole was used as corrosion inhibitor) into HNT. TEM result indicated the successful loading of benzimidazole into HNT. FTIR result confirmed the differences on the sharpness of some peaks as an evidence of benzimidazole loading into HNT. In addition, TGA

result showed the temperature of degradation of benzimidazole-loaded HNT was higher than pure HNT. Furthermore, EIS analysis showed that the coating resistance of benzimidazole loaded HNT-Epoxy reach $2.460E+07 \Omega$ of impedance value after 6 days of immersion, which indicated the good corrosion protection of proposed coating. It was proven that benzimidazole loaded HNT-Epoxy provided an active corrosion protection by releasing of benzimidazole in proper time to protect carbon steel surface against corrosion in 3.5wt% of NaCl solution.

References

- [1] E. Abdullayev, V. Abbasov, A. Tursunbayeva, et al., "Self-healing coatings based on halloysite clay polymer composites for protection of copper alloys," *ACS Applied Materials and Interfaces*, vol. 5, no. 10, pp. 4464-4471, April 2013.
- [2] A. Popoola, O. E. Olorunniwo, and O. O. Ige, "Corrosion resistance through the application of anti-corrosion coatings," *Developments in Corrosion Protection*, vol. 2, no. 12, pp. 241-270, February 2014.
- [3] D. G. Shchukin, S. V. Lamaka, K. A. Yasakau, M. L. Zheludkevich, M. G. S. Ferreira, and H. Mohwald, "Active anticorrosion coatings with halloysite nanocontainers," *The Journal of Physical Chemistry C*, vol. 112, no. 4, pp. 958-964, January 2008.
- [4] E. Abdullayev, R. Price, D. Shchukin, and Y. Lvov, "Halloysite tubes as nanocontainers for anticorrosion coating with benzotriazole," *ACS Applied Materials and Interfaces*, vol. 1, no. 7, pp. 1437-1443, June 2009.
- [5] Y. M. Lvov, D. G. Shchukin, H. Mohwald, and R. R. Price, "Halloysite clay nanotubes for controlled release of protective agents," *ACS Applied Materials and Interfaces*, vol. 2, no. 5, pp. 814-820, May 2008.
- [6] M. Liu, Z. Jia, D. Jia, and C. Zhou, "Recent advance in research on halloysite nanotubes-polymer nanocomposite," *Progress in Polymer Science*, vol. 39, no. 8, pp. 1498-1525, August 2014.
- [7] E. Abdullayev and Y. Lvov, "Clay nanotubes for corrosion inhibitor encapsulation: release control with end stoppers," *Journal of Materials Chemistry*, vol. 20, no. 32, p. 6681, August 2010.
- [8] A. Mobinikhaledi, N. Foroughifar, P. Mohammadlu, and M. Kalhor, "Synthesis of some benzimidazole-substituted benzotriazoles," *South African Journal of Chemistry*, vol. 61, no. 1, pp. 141-143, 2008.
- [9] N. Vijayan, G. Bhagavannarayana, R. Ramesh Babu, R. Gopalakrishnan, K. K. Maurya, and P. Ramasamy, "A comparative study on solution- and bridgman-grown single crystals of benzimidazole by high-resolution x-ray diffractometry, fourier transform infrared, microhardness, laser damage threshold, and second-harmonic generation measurements," *Crystal Growth Design*, vol. 6, no. 6, pp. 1542-2546, May 2006.
- [10] N. A. Abood and B. A. Saeed, "Structures and vibrational frequencies of imidazole, benzimidazole and its 2-alkyl derivatives determined by DFT calculations," *Basrah Journal of Science (C)*, vol. 30, no. 1, pp. 119-131, 2012.
- [11] M. F. Morks, P. Corrigan, N. Birbilis, and I. S. Cole, "A green MnMgZn phosphate coating for steel pipelines transporting CO₂ rich fluids," *Surface and Coatings Technology*, vol. 210, pp. 183-189, October 2012.
- [12] Zaki Ahmad, *Principles of corrosion engineering and corrosion control*. Elsevier Science & Technology Books, 2006.
- [13] Q. Bai and Y. Bai, *Subsea pipeline design*, 1st ed. Waltham: Elsevier, 2014, pp. 451-464.
- [14] D. Grigoriev, E. Shchukina, and D. G. Shchukin, "Nanocontainers for self-healing coatings," *Advanced Materials Interfaces*, vol. 4, no. 1, June 2016.
- [15] R. Meirowitz, "Microencapsulation technology for coating and lamination of textiles," *Smart Textile Coatings and Laminates*, vol. 3, no. 12, pp. 125-154, 2010.
- [16] M. Sauer, D. Streich, W. Meier, B. M. Sauer, D. Streich, and W. Meier, "pH-sensitive nanocontainers," *Advanced Materials*, vol. 13, no. 21, pp. 1649-1651, November 2001.
- [17] S. Simoes, J. Nuno Moreira, C. Fonseca, N. Duzgunes, and M. C. Pedroso De Lima, "On the formulation of pH-sensitive liposomes with long circulation times," *Advanced Drug Delivery Reviews*, vol. 56, no. 7, pp. 947-965, April 2004.
- [18] T. Y. Liu and Y. L. Lin, "Novel pH-sensitive chitosan-based hydrogel for encapsulating poorly water-soluble drugs," *Acta Biomaterialia*, vol. 6, no. 4, pp. 1423-1429, April 2010.
- [19] J. Qian and C. Berkland, "pH-sensitive triblock copolymers for efficient siRNA encapsulation and delivery," *Polymer Chemistry*, pp. 3472-3479, May 2015.
- [20] J. Gómez-estaca, R. Gavara, and P. Hernández-Muñoz, "Encapsulation of curcumin in electrosprayed gelatin microspheres enhances its bioaccessibility and widens its uses in food applications," *Innovative Food Science & Emerging Technologies*, vol. 29, pp. 302-307, May 2015.

- [21] K. M. Rao, K. S. V. K. Rao, G. Ramanjaneyulu, and C. S. Ha, "Curcumin encapsulated pH sensitive gelatin based interpenetrating polymeric network nanogels for anti-cancer drug delivery," *International Journal of Pharmaceutics*, vol. 478, no. 2, pp. 788-795, January 2015.
- [22] T. C. Lai, J. Yu, and W. B. Tsai, "Gelatin methacrylate/carboxybetaine methacrylate hydrogels with tunable crosslinking for controlled drug release," *Journal of Materials Chemistry B*, vol. 4, no. 13, pp. 2304-2313, April 2016.
- [23] Y. Guo et al., "RGD-decorated redox-responsive d- α -tocopherol polyethylene glycol succinate-poly(lactide) nanoparticles for targeted drug delivery," *Journal of Materials Chemistry B*, vol. 4, no. 13, pp. 2338-2350, April 2016.
- [24] M. Liu et al., "Functionalized halloysite nanotube by chitosan grafting for drug delivery of curcumin to achieve enhanced anticancer efficacy," *Journal of Materials Chemistry B*, vol. 4, no. 13, pp. 2253-2263, April 2016.
- [25] Y. Lv, L. Hao, W. Hu, Y. Ran, Y. Bai, and L. Zhang, "Novel multifunctional pH-sensitive nanoparticles loaded into microbubbles as drug delivery vehicles for enhanced tumor targeting," *Scientific reports*, vol. 6, p. 29321, April 2016.
- [26] I. Hofmeister, K. Landfester, and A. Taden, "PH-Sensitive nanocapsules with barrier properties: Fragrance encapsulation and controlled release," *Macromolecules*, vol. 47, no. 16, pp. 5768-5773, August 2014.
- [27] C. G. Dariva and A. F. Galio, "Corrosion Inhibitors - principles mechanisms and applications," *Developments in Corrosion Protection*, p. 16, 2014.
- [28] D. Gopi, E. M. Sherif, V. Manivannan, D. Rajeswari, M. Surendiran, and L. Kavitha, "Corrosion and corrosion inhibition of mild steel in groundwater at different temperatures by newly synthesized benzotriazole and phosphono derivatives," *Industrial & Engineering Chemistry Research*, vol. 53, no. 11, pp. 4286-4294, February 2014.
- [29] P. Yuan, D. Tan, and F. Annabi-Bergaya, "Properties and applications of halloysite nanotubes: recent research advances and future prospects," *Applied Clay Science*, vol. 112-113, pp. 75-93, August 2015.
- [30] E. Joussein, S. Petit, J. Churchman, B. Theng, D. Righi, and B. Delvaux, "Halloysite clay minerals -a review," *Clay Minerals*, vol. 40, no. 4, pp. 383-426, December 2005.
- [31] J. Zhang, J. Hu, J. Zhang, and C. Cao, "Studies of water transport behavior and impedance models of epoxy-coated metals in NaCl solution by EIS," *Progress in Organic Coatings*, vol. 51, no. 2, pp. 145-151, November 2004.
- [32] S. Masadeh, "Electrochemical impedance spectroscopy of epoxy-coated steel exposed to dead sea water," *Journal of Minerals and Materials Characterization and Engineering*, vol. 4, no. 2, pp. 75-84, October 2005.
- [33] M. Behzadnasab, S. M. Mirabedini, K. Kabiri, and S. Jamali, "Corrosion performance of epoxy coatings containing silane treated ZrO₂ nanoparticles on mild steel in 3.5 % NaCl solution," *Corrosion Science*, vol. 53, no. 1, pp. 89-98, January 2011.